ELSEVIER

MODIS Vegetation Index Compositing Approach: A Prototype with AVHRR Data

Wim J. D. van Leeuwen, Alfredo R. Huete,* and Trevor W. Laing**

In this study, the 16-day MODIS (MODerate resolution Imaging Spectroradiometer) vegetation index (VI) compositing algorithm and product were described, evaluated, and compared with the current AVHRR (Advanced Very High Resolution Spectroradiometer) maximum value composite (MVC) approach. The MVC method selects the highest NDVI (normalized difference vegetation index) over a certain time interval. The MODIS VI compositing algorithm emphasizes a global and operational view angle standardization approach: a reflectance-based BRDF (Bi-directional Reflectance Distribution Function) model, succeeded by a back-up MVC algorithm that includes a view angle constraint. A year's worth of daily global AVHRR data was used to prototype the MODIS vegetation index compositing algorithm. The composite scenarios were evaluated with respect to: 1) temporal evolution of the VI for different continents and vegetation types, 2) spatial continuity of the VI, 3) quality flags related to data integrity, cloud cover, and composite method, and 4) view angle distribution of the composited data. On a continental scale, the composited NDVI values from the MODIS algorithm were as much as 30% lower than the mostly, off-nadir NDVI results based on the MVC criterion. The temporal evolution of the NDVI values derived with the MODIS algorithm were similar to the NDVI values derived from the MVC algorithm. A simple BRDF model was adequate to produce nadir equivalent reflectance values from which the NDVI could be computed. Application of the BRDF and "back-up" components in the MODIS algorithm were dependent on geographic location and season, for example, the BRDF interpolation was most frequently applied in arid and semiarid regions, and during the dry season over humid climate vegetation types. Examples of a MODIS-like global NDVI map and associated quality flags were displayed using a pseudo color bit mapping scheme. ©Elsevier Science Inc., 1999

INTRODUCTION

Vegetation indices have been used effectively in numerous applications by scientists, government agencies, educational institutions, and private companies to conduct land cover classifications (Townshend et al., 1991; Roy, 1997), detect change, and derive biophysical properties of the vegetation such as fractional vegetation cover, biomass, leaf area index (LAI), fraction of absorbed photosynthetic active radiation (fAPAR), and phenology (Asrar et al., 1984; 1992; Baret and Guyot, 1991; Goward and Huemmrich, 1992; Justice et al., 1985; Sellers, 1985; Sellers et al., 1994). Vegetation indices also have been used to estimate net productivity (Tucker and Sellers, 1986; Running and Nemani, 1988; Prince, 1991), which has been related to biogeochemical cycles (Raich and Schlesinger, 1992) of vegetation and CO_2 sources and sinks (Fung et al., 1987; Tans et al., 1990).

Satellite systems, such as the AVHRR (Advanced Very High Resolution Radiometer) (Agbu et al., 1994) and SPOT4-VEGETATION (Systeme pour l'Observation de la Terre 4-VEGETATION) (Archard et al., 1994), SeaWiFS (Sea-Viewing Wide Field-of-View Sensor) (Hooker et al., 1992), and soon to be launched MODIS-EOS (MODerate resolution Imaging Spectroradiometer—Earth Observing System) (Salomonson et al., 1989; Justice et al., 1998), and GLI (Global Imager) (Nakajima et al., 1998), acquire global bidirectional radiance data of the Earth's surface under different solar illumination angles. After applying atmospheric corrections and processing the radiance data into surface reflectance data, these satellite

* Department of Soil, Water, and Environmental Science, University of Arizona, Tucson

Address correspondence to Wim J. D. van Leeuwen, Univ. of Arizona, Dept. of Soil, Water, and Environmental Science, 1200 E South Campus Dr., Room 429, Tucson, AZ 85721. E-mail: leeuw@ag.arizona.edu

Received 6 October 1998; revised 16 February 1999.

REMOTE SENS. ENVIRON. 69:264–280 (1999)

655 Avenue of the Americas, New York, NY 10010

0034-4257/99/$–see front matter
PII S0034-4257(99)00022-X

systems capture the strong anisotropic reflectance properties that vary with land cover type, relative amounts of characteristic vegetation and soil components within each pixel, and Sun–Earth–sensor geometry. Therefore, some knowledge of the bidirectional reflectance distribution function (BRDF) is a requirement for successful utilization of directional reflectance data and vegetation indices, and the derivation of land cover-specific biophysical parameters (Cihlar et al., 1994a). However, due to frequent cloud cover and sensor–Sun–Earth geometric characteristics, the reflectance data needs to be composited in time and space to allow for temporal and spatial continuous monitoring of surface soil and vegetation dynamics with vegetation indices.

AVHRR (1.1 km at nadir), SeaWiFS (1.13 km at nadir), and MODIS (250 m and 500 m at nadir) are whiskbroom sensors, causing the pixel size to increase with scan angle by as much as a factor of 4. GLI (250 m and 1km) and SPOT4-VEGETATION (1 km) are pushbroom sensors which have equal pixel sizes across all scan angles. The satellite specific features associated with the spatial resolution of each pixel need to be considered when vegetation indices (VIs) are composited over time. The 16-day repeat cycle of MODIS and the variable pixel sizes during these 16 days will affect the interpretation of remote sensing products derived from bidirectional reflectance factor (BRF) data and can be a source of error because the BRDF characteristics of large pixels are not necessarily the same as those of small pixels (van Leeuwen et al., 1997a). The pixel size becomes an important variable in evaluating anisotropic and biophysical properties of both heterogeneous and homogeneous land surfaces.

The influence of variable Sun–target–sensor configurations on derived vegetation indices can be standardized in various manners, including: 1) Standardize reflectances to nadir view angle at a solar zenith angle representative of the observations; 2) standardize reflectances to nadir view angle and a temporally and globally constant solar zenith angle; 3) adjust to a constant "off-nadir" view angle with a constant sun angle; or 4) use of spectral (bihemispherical) albedos. For the standard MODIS VI products, we propose to use the first method (Justice et al., 1998) and examine the other three approaches postlaunch. Preliminary analysis (Huete et al., 1997) suggests that both the third and fourth approaches may enhance vegetation detection only over a limited range of land cover conditions (Kimes et al., 1984; Privette et al., 1996), and will result in overall decreased sensitivity from desert to forest, and present greater saturation problems in more densely vegetated canopies.

The objectives of this research were: a) to present the current status of the 16-day/250 m MODIS vegetation index compositing algorithm, b) to evaluate the MODIS vegetation index compositing algorithm in comparison with the "maximum value composite" algorithm, and c) to prototype the MODIS vegetation index product with AVHRR data. In this study, the global spatial and temporal aspects of the compositing results were emphasized. Additional detailed VI compositing results for individual pixels and specific vegetation types will be presented in future communications.

The MODIS-VI will not be completely the same as the VI derived from the NOAA-AVHRR instrument due to different sensor characteristics. The position and width of the "common" MODIS and AVHRR spectral bands are quite different. Both the MODIS red (620–670 nm) and near-infrared (NIR; 841–876 nm) spectral bands are much narrower than the AVHRR red (580–680 nm) and NIR (725–1100 nm) bands, causing differences in the spectral response of vegetation canopies with consequent differences in vegetation index response (Teillet et al., 1997). The narrower widths of the MODIS spectral bands eliminate the water absorption regions (around 950 nm and 1100 nm) in the NIR and also render the red band more sensitive to chlorophyll absorption.

The atmospheric correction and cloud-screening approach to be used for MODIS are both significantly improved over the AVHRR approach. The experience of working with AVHRR data aided notably in the development of the MODIS product algorithms. In the following sections we demonstrate why the maximum VI value composite (MVC) approach is less desirable for compositing MODIS data.

Maximum Value Composite (MVC) Scenario

The currently accepted procedure for generation of composited AVHRR-NDVI (normalized difference vegetation index) products is the maximum value composite (MVC) technique (Holben, 1986). The MVC selects the maximum NDVI value on a per-pixel basis over a set compositing period and is designed to minimize atmospheric effects, including residual clouds. The compositing procedure generally includes cloud screening and data quality checks (Goward et al., 1994; Eidenshink and Faundeen, 1994).

The MVC works nicely over near-Lambertian surfaces where the primary source of pixel variations within a composite cycle is associated with atmosphere contamination and path length. However, the MVC becomes inconsistent and unpredictable due to anisotropic properties of vegetated canopies and varying atmospheric conditions. The bidirectional spectral behavior of numerous, "global" land cover types and terrestrial surface conditions have been widely documented and shown to be highly anisotropic due to canopy structure, shadowing, and background contributions. (Kimes et al., 1985; van Leeuwen et al., 1994; Vierling et al., 1997). Ratioing of the NIR and red spectral bands to compute vegetation indices does not remove surface anisotropy (Walter-Shea et al., 1997). This is a result of the spectral dependence of the BRDF, with the NIR reflectance response gener-

ally more anisotropic than the red reflectance response (Gutman, 1991; Roujean et al., 1992). The MVC approach becomes even less appropriate with atmospherically corrected data sets, since the anisotropic behavior of vegetation indices is stronger (Cihlar et al., 1994b).

The MVC method works best for data uncorrected for atmosphere (Cihlar et al., 1994a), although numerous inconsistencies result (Gutman, 1991; Goward et al., 1991; 1994; Cihlar et al., 1994b; 1997). The MVC favors cloud-free pixels, but does not necessarily pick the pixel closest to nadir or with the least atmospheric contamination. Although the NDVI tends to increase for atmospherically corrected data, it does not mean that the highest NDVI is an indication of the best atmospheric correction. Many studies and experiments have shown the maximum NDVI approach to select pixels with large view and sun angles which are not always cloud-free or atmospherically clear (Goward et al., 1991; Moody and Strahler, 1994; Cihlar et al., 1994b; 1997). Since residual clouds and sun and view angles alter the surface reflectances and thus the VIs, comparisons of global vegetation types would not be consistent throughout the year.

Fundamentally, the MVC is not appropriate for the atmospherically corrected surface reflectance data and vegetation indices to be generated by MODIS algorithms for several reasons. In the EOS era, surface anisotropy and bidirectional reflectances will become more pronounced as a result of improved atmospheric removal algorithms (Vermote et al., 1997a,b), which will accentuate differences in surface bidirectional reflectances resulting from canopy structural influences (Cihlar et al., 1994a). VIs computed from atmospherically corrected surface reflectance data will therefore be strongly biased toward off-nadir viewing and larger solar zenith angles, where more vegetation is viewed or illuminated by the sensor. In addition, the atmospheric correction is less accurate at off-nadir view angles if the coupling between the BRDF and the downward radiance at the surface level is not taken into account (Vermote et al., 1997a). Pixels with off-nadir viewing angles also have more distortions and are coarser in size, that is, less detail. Furthermore, the MVC method will overestimate NDVI values, which will result in an overestimation of vegetation biophysical parameters and will contribute to the saturation of the NDVI.

The MVC criterion applied to MODIS data will thus result in the selection of off-nadir, distorted, and less radiometrically accurate pixels, and deviate from the primary goal of working with the finest (nominal) resolution 250-m NDVI data sets. BRDF corrections of AVHRR reflectances to a standard nadir view angle have been shown to improve the accuracy of the composited NDVI (Roujean et al., 1992; Cihlar et al., 1994a; Wu et al., 1995). Therefore, the MODIS compositing criteria will be weighted more toward angular considerations. This is done by incorporating a BRDF compositing approach, which has the goal to standardize the VI to nadir view and representative or constant solar angles. The MVC algorithm will be used as a "backup" composite scenario in case a BRDF correction cannot be applied and if the MODIS atmospheric correction and the MODIS cloud mask are found or reported to be inaccurate.

There are other alternatives to simply choosing the highest NDVI value over a compositing cycle. One may integrate or average all cloud-free pixels over the period. Meyer et al. (1995) demonstrated the importance of the effect of surface anisotropy and Sun/sensor geometry on the NDVI from AVHRR, and suggested that averaging the NDVI was superior to the MVC approach. The best index slope extraction (BISE) (Viovy et al., 1992) method reduces noise in NDVI time series by selecting against spurious high values and through a sliding compositing cycle. Use of the thermal channel has also been shown to be helpful. Knowledge of the ecological evolution of a land cover with respect to a VI temporal response might also be of use for the improvement of compositing techniques (Viovy et al., 1992; Qi et al., 1994; Moody and Strahler, 1994). This will not be used for the initial MODIS compositing algorithm due to the advanced knowledge required of the dynamics of land cover growth patterns, seasonality, and response to climate change (precipitation, temperature). The use of land cover specific optimized composite scenarios would also introduce discontinuities, but might perform better on a regional scale since more *a priori* knowledge can be incorporated with respect to the choice of BRDF models, vegetation cover type, climate, and landscape dynamics. Other VI compositing techniques are discussed by Cihlar et al. (1994b) and Qi and Kerr (1997).

MODIS Vegetation Index Compositing Goals and Considerations

The MODIS vegetation index composite scenario was developed within the EOS (Earth Observing System) framework of providing more accurate products to monitor changes in the Earth system.

The main MODIS VI compositing goals are to:

- provide accurate and cloud-free vegetation index (VI) imagery over set temporal intervals,
- maximize global and temporal land coverage at the finest spatial and temporal resolutions possible,
- standardize variable sensor view and sun angles,
- ensure the quality and consistency of the composited data,
- depict and reconstruct phenological variations,
- accurately discriminate interannual variations in vegetation.

With the aforementioned compositing goals in mind, the following considerations are also of importance in the design of the MODIS vegetation index compositing algorithm:

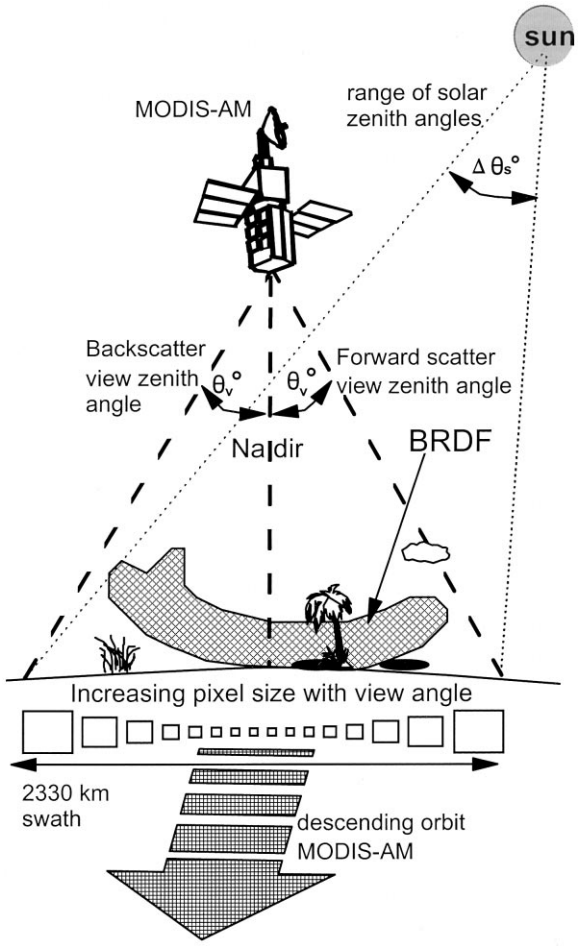

Figure 1. Illustration of MODIS data acquisition on the EOS-AM platform (not to scale). The bidirectional reflectance distribution function (BRDF) changes with view and sun geometry. Notice the shadow caused by clouds and canopy. MODIS pixel dimensions, cross-track and along-track, change with scan angles: 0°—250 m× 250 m; 15°—270 m×260 m; 30°—350 m×285 m; 45°—610 m×380 m (computed for the fine resolution red and NIR detectors; 250 m at nadir on the ground).

- The pixels with the smallest view zenith angle will have the finest spatial resolution. This is 250 m for the red and NIR detectors. Realistically, the 250 m pixel size will increase to over 1 km across track at the edges of the scan (55°) and up to 500 m along track (Fig. 1).
- Spatial degradation and blurring increase greatly with off-nadir view angles (Moody and Strahler, 1994), and off-nadir pixels will thus be more difficult to register than nadir pixels.
- Established biophysical parameter relationships with vegetation indices are based upon nadir-viewing angles.
- Vegetation index "saturation" problems become greater with off-nadir view and larger solar zenith angles.

Critical to the quality of the NDVI product will be the coregistration of the red and NIR 250m channels, spectral stability of the channels, pixel registration (Townshend et al., 1992), and calibration over time (Price, 1987). Actual day-to-day registration accuracy over a set composite period (16 days) will be determined postlaunch. The MODIS data characteristics, process stream, and the vegetation index algorithm and rationale are further described in the following sections.

MODIS VI and BRDF

Vegetation indices are affected by variations in bidirectional reflectance factors, which vary greatly as a function of Sun–target–sensor geometries (Walter-Shea et al., 1997). Figure 1 gives a schematic diagram of the position of the sun and MODIS sensor for the EOS-AM1 morning overpass and descending node. MODIS will image the Earth's surface over a swath width of 2330 km over sensor viewing angles of ±55° cross-track, with the effective view angle on the ground being slightly larger owing to the Earth's curvature. The pixel size is increasing with view angle. Solar zenith angles across MODIS imagery may vary up to 20° from edge to edge of the 2330 km swath and also vary spatially with latitude and seasonally over the growing season. The backscatter direction of the MODIS swath has larger solar zenith angles than the forward scatter (Fig. 1). Since the NDVI tends to increase with both larger view and larger solar zenith angles, the resulting variability in both view and solar zenith angles are important for intercomparison of vegetation covers at different latitudes and in different seasons, and should be considered in the VI compositing algorithm if we are to maintain "global" VI robustness. BRDF model parameters can be used to normalize and interpolate the surface reflectance to nadir view angles. However, the sun angle variability will be minimally incorporated in the BRDF correction, since the data necessary to standardize to a certain sun angle for each composite time interval (16 days in the case of MODIS) is very limited, and thus would be less accurate outside of the observed sun angle range. More research is needed to determine the most accurate method to extrapolate satellite observations to a standard sun angle throughout the year. Therefore, the solar zenith and azimuth angles should be included with the composited data (reflectance and vegetation index data) to be used for postprocess standardization of the vegetation indices.

Numerous canopy bidirectional reflectance distribution function (BRDF) models have been developed to account for the anisotropy in land reflectances as a function of view and solar zenith angles. However, a BRDF model must be robust and operational on a global scale. Our approach is to use the simple Walthall model (Walthall et al., 1985) to standardize the reflectance data to nadir and compute nadir-based VIs. This has been shown

to be far superior than a maximum NDVI (MVC) approach (van Leeuwen et al., 1996). Cihlar et al. (1994a) successfully used the Walthall model with AVHRR data for a range of vegetation types at a regional scale. The BRDF approach estimated nadir-equivalent VIs better than the MVC, which overestimated the nadir-equivalent NDVI.

The results from the BRDF approach are also thought to best represent the state of the land surface by involving several cloud-free observations. However, the 16-day repeat cycle of MODIS can result in variable BRDF characteristics (van Leeuwen et al., 1997a) because the multiangle reflectance values are acquired from pixels that vary in size during these 16 days (Fig. 1). In this case, the uncertainty in the VI will depend on spatial resolution and the angle distribution at which the data were obtained, the heterogeneity of the surface area, and the choice of BRDF model (van Leeuwen et al., 1997a). Increasing degradation of the spatial resolution with off-nadir view angles will minimally affect the nadir-interpolated reflectance values and resulting VI values if the multiangular observations are equally distributed in view angle space (van Leeuwen et al., 1997a). Nadir-equivalent reflectance retrievals for fallow and Aspen vegetation, using the Walthall model and simulated MODIS pixel size degradation for the 250 m at nadir detectors, introduced an uncertainty in the NDVI of 0.011 and 0.008 respectively (van Leeuwen et al., 1997a). Off-nadir spatial degradation will impact the MODIS 1 km and coarser VI products less since the input to these products are based on finer resolution (250 m and 500 m) data sets that are aggregated to 1 km.

Privette et al. (1997) compared many linear models as described by Wanner et al. (1997), and found that nadir interpolation was best achieved with the Ross-thick/Li-sparse BRDF model over many vegetation types [data sets collected with the PARABOLA (Portable Apparatus for Rapid Acquisition of Bidirectional Observations of Land and Atmosphere)] (Deering and Leone, 1986). van Leeuwen et al. (1996) found the Walthall model to perform best for nadir-equivalent vegetation indices for most vegetation types [Advanced Solid State Array Spectroradiometer (ASAS) data sets]. The Walthall model was found to work equally well as Roujean's BRDF model. The Ross-thick/Li-sparse BRDF model caused a few outliers when used in the forward modeling mode to derive nadir reflectance values. Experience with ASAS and AVHRR data showed the Walthall model to be more robust than most of the other linear models. The Walthall model also requires the least number of floating operations per pixel, which is an important consideration in the production of a global VI product at 250 m resolution and 16-day temporal intervals.

Compositing Period

Variable composite periods have been used to obtain cloud-free NDVI data on a global scale. The minimum compositing period is limited by cloud cover frequency and may vary from every 5 days at higher latitudes to as long as 30 days or more in some humid tropical areas. NDVI composite periods have varied among 7, 9, 10, 11 and 14 days and monthly intervals with variable (1 km to 1°) spatial resolutions (Townshend, 1994). The composite period depends on its application and the availability of cloud free data on a global scale. Shorter compositing periods will pick up more dynamic land cover changes and allows one to combine compositing periods to monthly or biweekly periods. However, the shorter the compositing period, the greater the likelihood of cloud-affected or missing pixels in the composited image. The 16-day MODIS compositing cycle was designed according to the EOS-AM1 16-day repeat cycle and consequent attainment of the full array of viewing angles. This seems appropriate since it provides the opportunity to avoid clouds as well as to cover all latitudes within a range of small viewing angles. The monthly compositing cycle is based on demand and heritage of the user community.

It is unclear if the nadir AVHRR repeat cycle of approximately 9 days versus the 16 days of MODIS will affect the derivation of nadir-equivalent reflectance values from BRDF models for either sensor. Based on the repeat cycle, more nadir AVHRR then nadir MODIS observations are possible within a 16-day period. The 2700-km swath width of AVHRR will result in a larger view angle range compared to the 2330-km swath width of MODIS. Furthermore, the AM overpass of MODIS results in less cloud cover in comparison to the cloudier afternoon overpass of the AVHRR. Since data from both sensors will have random dropouts of observations due to clouds, the distribution and range of view angles will be different, but not likely to affect the final nadir-equivalent VI product significantly. The expected retrieval accuracy of bidirectional reflectance values over land for MODIS angular sampling are reported by Lucht (1998) and Wanner et al. (1997).

MODIS Data Stream

MODIS products that are relevant to the vegetation index are shown in Figure 2. The MODIS data streams [top of the atmosphere (TOA) calibrated radiance, cloud mask, atmospheric correction and surface reflectance, vegetation indices] are set up to flow into the product algorithms in a predetermined order. For a tractable and best solution to the compositing algorithm, it was logical to input the atmospherically corrected surface reflectance data in combination with the cloud mask and use as many "good" observations as possible during a composite period. This runs counter to the MVC scenario based on nonatmospherically corrected reflectance data as suggested by Cihlar et al. (1994a) for the AVHRR data. If changes in the vegetation index compositing algorithm call for a different processing scenario, significant changes in the EOS production system can be required, including hardware, software, and networking redesign and implementation.

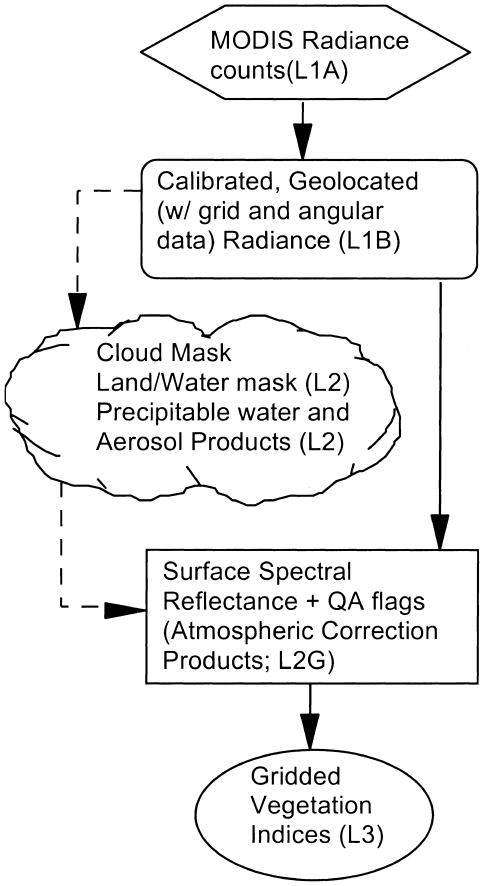

Figure 2. Flow diagram showing the relationship of relevant MODIS land and atmosphere products (Level 1—L1; Level 2—L2; Gridded L2–L2G; Level 3—L3) that are required to generate the gridded, composited vegetation indices.

MODIS Vegetation Index Products

Two gridded vegetation indices will be produced, the normalized difference vegetation index (NDVI) and the enhanced vegetation index (EVI), both with quality assurance (QA) flags that indicate the quality of the VI product and input data [Eqs. (1) and (2)]:

$$\mathrm{NDVI}=(\rho_{\mathrm{NIR}}-\rho_{\mathrm{red}})/(\rho_{\mathrm{NIR}}+\rho_{\mathrm{red}}), \quad (1)$$

$$\mathrm{EVI}=2.5(\rho_{\mathrm{NIR}}-\rho_{\mathrm{red}})/(L+\rho_{\mathrm{NIR}}+C_1\rho_{\mathrm{red}}-C_2\rho_{\mathrm{blue}}), \quad (2)$$

where ρ_λ is the surface reflectance factor for the presented wavelengths (λ= red, NIR, and blue). The enhanced VI is described by Huete et al. (1997) and is designed to improve sensitivity to a wider, global range of vegetation conditions and better depict vegetation canopy structural parameters, such as LAI. L is the canopy background adjustment factor, and C_1 and C_2 are weight coefficients which adjust for atmospheric aerosol effects. Prior to MODIS-launch, L, C_1, and C_2 are currently approximated by 1, 6, and 7.5, respectively. Another enhancement to the VIs could be made by the replacement of the red reflectance band with the middle infrared (MIR)spectral reflectance values to allow for vegetation monitoring during heavy aerosol conditions (Miura et al., 1998). van Leeuwen et al. (1996) showed the new and improved VIs to be more sensitive to angular effects and that a maximum value of these enhanced indices may exaggerate a bias towards off-nadir view angles.

The MODIS VI products will be spatially and temporally resampled, designed to provide cloud-free vegetation index maps at nominal resolutions of 250 m, 1 km, and 25 km. The latter is also known as the climate modeling grid (CMG). The composited surface reflectance data from each pixel will be used to compute both the NDVI and the EVI gridded products at 1 km and 25 km spatial resolutions. The 250 m MODIS VI product will only contain the NDVI, since the red and NIR bands are the only bands at 250 m resolution. The gridded VIs will be produced at 16-day and monthly temporal resolutions. Table 1 gives an overview of the VI product characteristics.

The MODIS land team will use a diverse set of validation techniques to develop uncertainty information on its products. The methods include comparisons with field data collected over a globally distributed set of validation test sites, comparisons with data and products from other sensors, analysis of trends in MODIS land products, and analysis of process model results. The results of the validation activities will be communicated to the end-user through both published literature and quality assessment metadata accompanying the product data sets (Morisette et al., 1998).

MODIS VI Composite Algorithm

The logic of the compositing algorithm is based on the MODIS specific input data and theoretical knowledge of radiative transfer and surface reflectance anisotropy. The compositing algorithm will optimize the choice of the best VI representative for each composite period, spatial resolution, and global land extent. The compositing algorithms will rely on information from the cloud mask (Ackerman et al., 1996), atmospheric correction (Vermote, 1997a), view zenith angle, solar zenith angle, relative azimuth angle, georegistration (Wolfe et al., 1998), and surface BRDF normalization. The algorithms utilize the information in the reflectance-quality assurance (QA) flags, partially derived from the MODIS cloud mask product, to preprocess the atmospherically corrected reflectance data of MODIS Bands 1, 2, 3, and 7 (red, NIR, blue, MIR) over land only. Land pixels with clouds, shadow, and bad data integrity will be excluded from the VI composite.

The MODIS algorithm selects all the reflectance data for a 16-day period, based on data integrity and cloud flags, and fits the Walthall BRDF model to the individual band data. The empirical BRDF model developed by Walthall et al. (1985) [Eq. (3)] is used to derive nadir reflectance data for each pixel and 16-day intervals:

$$\rho_\lambda(\theta_v, \varphi_s, \varphi_v)=a_\lambda\theta_v^2+b_\lambda\theta_v\cos(\varphi_v-\varphi_s)+c_\lambda, \quad (3)$$

Table 1. MODIS Vegetation Index Product Characteristics, Including Temporal and Spatial Resolutions and the Current Data Fields for Each Data Product[a]

MOD13	*Temporal Resolution*	*Spatial Resolution*	*Data Fields*
A1	16 days	250 m	NDVI, QA(16), ρ_{NIR}, θ_v, θ_s, $(\varphi_s-\varphi_v)$
A2	16 days	1 km	NDVI, EVI, $QA_{NDVI}(16)$, $QA_{EVI}(16)$, ρ_{red}, ρ_{NIR}, ρ_{blue}, ρ_{MIR}, θ_v, θ_s, $(\varphi_s-\varphi_v)$
A3	Monthly	1 km	NDVI, EVI, $QA_{NDVI}(16)$, $QA_{EVI}(16)$, ρ_{red}, ρ_{NIR}, ρ_{blue}, ρ_{MIR}, θ_v, θ_s, $(\varphi_s-\varphi_v)$
C1	16 days	CMG	NDVI, EVI, $QA_{NDVI}(8)$, $QA_{EVI}(8)$, ρ_{red}, ρ_{NIR}, ρ_{blue}, ρ_{MIR}, θ_v, θ_s, $(\varphi_s-\varphi_v)$, $mean_{NDVI}$, std_{NDVI}, $mean_{EVI}$, std_{EVI}, % cloud cover, % vegetation cover
C2	Monthly	CMG	NDVI, EVI, $QA_{NDVI}(8)$, $QA_{EVI}(8)$, ρ_{red}, ρ_{NIR}, ρ_{blue}, ρ_{MIR}, θ_v, θ_s, $(\varphi_s-\varphi_v)$,

[a] In the sweep of MODIS data products, all vegetation index products are referred to by MOD13 (MODIS product # 13). MOD13C1 will also carry the CMG statistical mean and standard deviation (std) of the NDVI and EVI, % cloud cover for each CMG pixel, and % vegetation cover based on a VI threshold. These statistics will all be computed from the 1 km subgrid data, which is the input to the CMG pixels. All data will be stored in 2-byte integers, except for the quality assurance (QA) flags which are stored in both 16- and 8-bit words, as indicated by the numbers in brackets behind "QA" in the table.

where the atmospherically corrected reflectance (ρ_λ) values for the appropriate wavelengths (λ; i.e., red, NIR, blue) are modeled as a function of the view zenith angle (θ_v), and sun (φ_s) and view (φ_v) azimuth angles. The model parameters a_λ, b_λ, and c_λ are obtained using a least squares curve fitting procedure. "c_λ" is equal to the reflectance at nadir view angle. The prevalent sun angle and VIs will be computed from the composited and normalized surface reflectance observations. Based on our experience with AVHRR and ASAS data, a minimum of five surface reflectance observations are currently required for a stable BRDF model (Walthall's) inversion. Nadir interpolated values were rejected when the resulting reflectance values were negative or when the NDVI was higher than the MVC based NDVI ($NDVI_{BRDF}>NDVI_{MVC}$). If observations during a 16-day interval are unequally distributed in view angle space (e.g., backscatter observations only) or unequally affected by undesirable atmospheric conditions (e.g., smoke, clouds), negative nadir reflectance values can be derived from the BRDF model. Negative reflectance values can also be generated if inaccurate atmospheric parameters (e.g., aerosol optical thickness) are used to realize atmospheric corrections.

Since not all pixels will have five or more cloud-free data points during a 16-day period, a back-up algorithm is used which selects the highest NDVI based on two cloud-free pixels with their view angles closest to nadir. The absolute view zenith angle is taken for all cloud-free pixels, after which their view angles are sorted in ascending order. The NDVI is computed for the observations with the two smallest view zenith angles, after which the MVC rule is applied and the most optimal observation selected. This will be referred to as the constraint view angle, maximum value composite (CV-MVC) approach. If only one cloud-free observation is available over the composite period, this observation will automatically be selected to represent the composite period. If all data during a 16-day period were affected by clouds, based on the cloud flags, the view angle constraint for the MVC method will be released; and the VI will be calculated for all days, and the best pixel chosen based on the maximum value of the NDVI among all observations.

The 16-day 250 m and 1 km VI products (MOD13A1 and MOD13A2; MODIS VI product numbers 13A1 and 13A2; Table 1) will each be produced with similar algorithms as described in previous sections. Monthly and spatially aggregated (climate modeling grid resolution-CMG- 25 km) VI products (MOD13A3, MOD13C1, and MOD13C2; Table 1) will be based on the 16-day/1-km VI product. It must be noted that the 16-day products do not run in sync with the beginning of each calendar month. The monthly VI product (monthly products are composited by calendar month) will be based on the time-weighted average of the two to three 16-day products that contribute to each month. The CMG resolution will be the mean of all "good" 1-km composited reflectance data, after which the VIs will be computed. More detailed descriptions are given by Huete et al. (1999).

Numerical and Programming Considerations

A least-squares solution for the Walthall BRDF model parameters requires that a 3-variable system of linear equations be solved. This is achieved through a partial-pivoting matrix inversion, performed by a standard decomposition/back-substitution procedure. In the case of the Walthall BRDF model, where the parameter c is defined as the nadir reflectance value, the other two parameters do not need to be explicitly solved. The nadir approximation can then be directly determined through forward Gaussian elimination rather than a complete matrix inversion at a substantial savings in floating point operations.

DATA AND METHODS

Prelaunch MODIS VI Prototype with AVHRR Data

One year (1989) of daily Pathfinder AVHRR data over land (James and Kalluri, 1994) was obtained from the GSFC-DAAC (Goddard Space Flight Center–Distributed Active Archive Center) to test and prototype the MODIS vegetation index compositing. The daily Pathfinder data

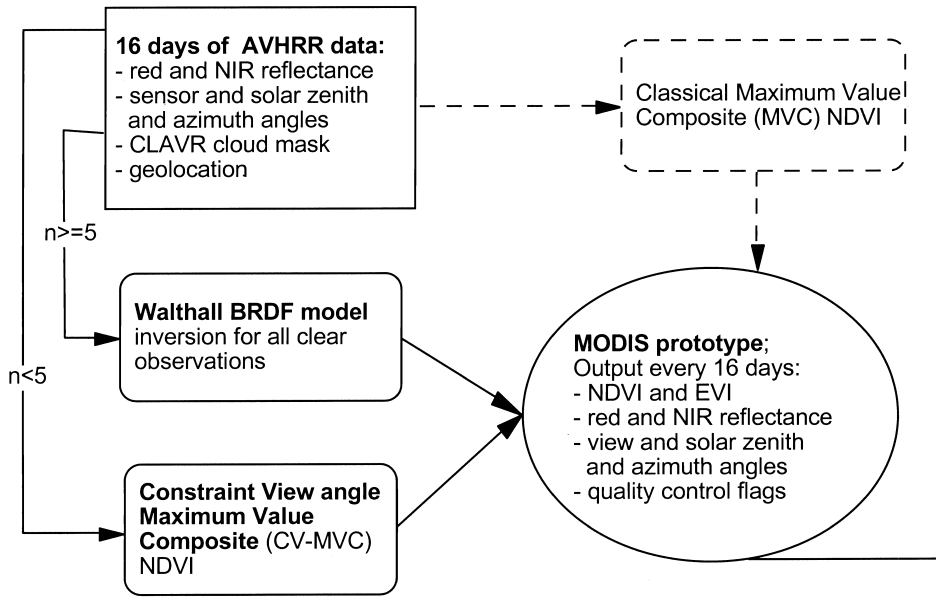

Figure 3. Diagram showing the sequence of MODIS prototype processing steps for compositing of AVHRR test data sets.

is mapped to a global 8 km equal area grid using the Goode Interrupted Homolosine projection, resulting in global spatial dimensions of 5004 by 2168 pixels (columns and rows). The AVHRR data was in the Hierarchical Data Format (HDF) and consisted of 12 data fields: NDVI, CLAVR (cloud algorithm for AVHRR) cloud flags, quality assurance flags, scan angle, solar zenith angle, relative azimuth angle, Channel 1 reflectance, Channel 2 reflectance, Channel 3 brightness temperature, Channel 4 brightness temperature, Channel 5 brightness temperature, date and hour of the observation. The reflectance data were already corrected for Rayleigh scattering and ozone absorption. Cloud flags were produced by NOAA's cloud algorithm for AVHRR (CLAVR) (Stowe et al., 1991). The land/sea mask was an ancillary data layer used in the processing. More specific information on the Pathfinder AVHRR land data can be found in the *User's Manual* (Agbu and James, 1994).

The daily AVHRR data was processed to prototype and compare the MODIS and MVC vegetation index compositing algorithms (Fig. 3) for the MODIS era. Slight adjustments were made to incorporate the AVHRR cloud mask, as opposed to the MODIS cloud mask, to facilitate the MODIS VI prototype with AVHRR data. The quality assurance (QA) flags for a global NDVI composite using a BRDF approach included eight flags (one bit per flag) related to: data integrity (1); land/water mask (2); the applied MODIS composite approach (3–5) (BRDF, CV-MVC, MVC); and the cloud mask (6–8) (cloudy, mixed cloudy/clear, shadow). The actual MODIS QA flags will have additional information about the atmospheric correction methodology and atmosphere aerosol and water vapor characteristics. More detailed information regarding QA fields can be found through several web sites (Huete et al., 1999; http://modland.nascom.nasa.gov/QA_WWW/modland-specs.html). The VI composite prototype output consisted of the following data fields: NDVI, QA (8), ρ_{red}, ρ_{NIR}, θ_v, θ_s, $(\varphi_s-\varphi_v)$. Note that the MODIS 250-m/16-day NDVI product (Table 1) will not include the red reflectance observations. This was to reduce the volume of the data that needs to be archived. The red reflectance data, however, can be retrieved using the relationship between NDVI and ρ_{NIR} [Eq. (4)]:

$$\rho_{red}=(\rho_{NIR}-\rho_{NIR}\ \text{NDVI})/(1+\text{NDVI}). \quad (4)$$

The relative differences [100 $(\text{NDVI}_{MVC}-\text{NDVI}_{MODIS})/\text{NDVI}_{MVC}$] between the MODIS composite approach and MVC were computed globally and for the areas where different composite methodologies (BRDF as opposed to CV-MVC; constraint view angle MVC) were applied.

RESULTS AND DISCUSSION

Global Temporal VI Profiles

Applying the MODIS and MVC compositing algorithms to 1 year of daily AVHRR data resulted in 23 consecutive global composites of the NDVI. The mean global NDVI_{MODIS} and NDVI_{MVC} values were obtained for all pixels, composite periods, and different MODIS compositing scenarios. Figure 4a shows the globally averaged temporal profiles of the mean NDVI values derived from the MODIS algorithm (NDVI_{MODIS}) and the mean NDVI values derived from the MVC algorithm (NDVI_{MVC}). The temporal profile of the NDVI_{MODIS} was always lower than the NDVI_{MVC} as shown in Figure 4a. Globally, the NDVI_{MODIS} was between 5% and 8% lower then the NDVI_{MVC} (Fig. 4a).

Using the QA information, for each pixel where the BRDF model was applied, the MVC was computed as

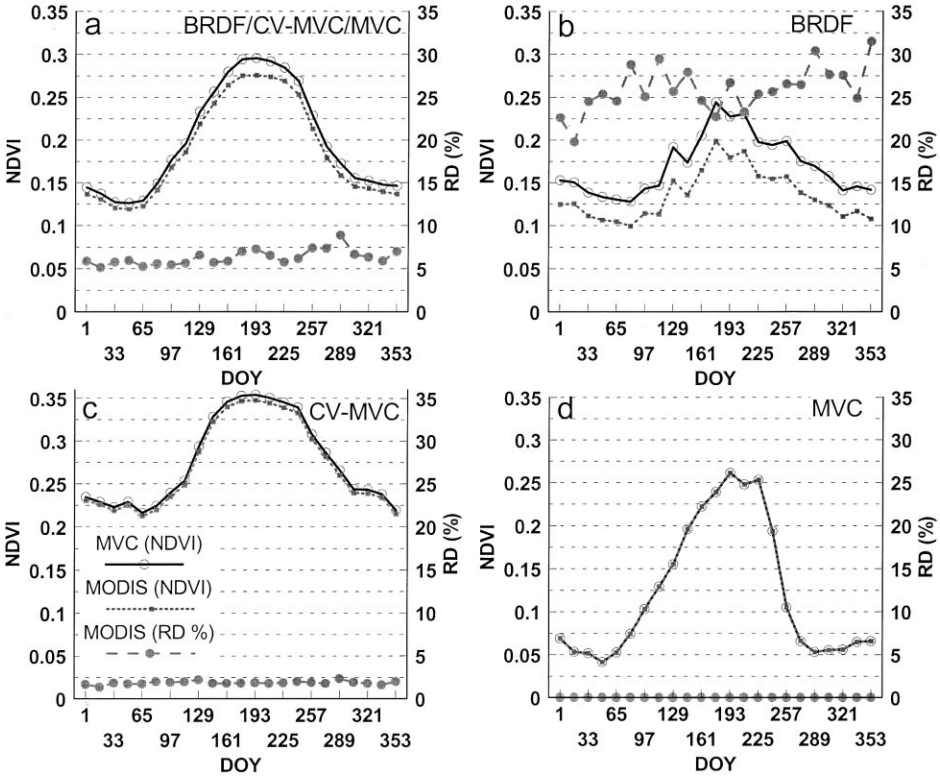

Figure 4. Temporal comparison of the global mean $NDVI_{MVC}$ and the mean $NDVI_{MODIS}$ as well as the temporal development of the percent relative difference (RD) between MVC and MODIS. The fractions of pixels for which the relative differences were computed are given in Figure 5. The MODIS results were separated based on the applied composite method. For example, for all the pixels where the BRDF was applied, the MVC was computed as well to make the comparison: a) results for MVC and $MODIS_{BRDF/CV-MVC/MVC}$ algorithms, including all pixels; b) results for MVC and $MODIS_{BRDF}$ algorithm; c) results for MVC and $MODIS_{CV-MVC}$ algorithm; d) results for MVC and $MODIS_{MVC}$ algorithm.

well and the relative difference computed for these pixels. Figure 4b shows the temporal profile of the mean of all the NDVI values standardized to nadir with the equivalent mean $NDVI_{MVC}$ results. Thus, whenever the MODIS-BRDF was applied, the resulting NDVI values were between 20% and 30% lower than the $NDVI_{MVC}$ (Fig. 4b). The variability of the BRDF and MVC derived temporal NDVI profiles are likely due to the fact that the compositing algorithm is applied and averaged over different geographic locations and land cover types, depending on the cloud cover distribution in time and space during each composite period.

When we compare the areas where $NDVI_{MODIS,\ CV-MVC}$ was applied with $NDVI_{MVC}$, we find only slight differences (Fig. 4c). $NDVI_{MODIS,\ CV-MVC}$ results were 1–2% lower than the $NDVI_{MVC}$ results throughout the year. As expected, there were no differences between the $NDVI_{MODIS}$ and the $NDVI_{MVC}$ values, when the MODIS composite was forced to select the maximum NDVI value (Fig. 4d). MODIS only utilizes MVC over "cloudy" observations. It is interesting to note, however, that the "cloudy" NDVI values had a very clear multitemporal profile, indicating that the cloud mask or integrity flags might be too restrictive. Since MODIS will acquire data over less cloudy conditions (morning overpass), we expect the "global" relative difference (RD) between the MODIS and MVC derived NDVI values to approach those of the BRDF results (20–30%) (Fig. 4b). It should be noted that the temporal profiles of the $NDVI_{BRDF}$ are fairly low compared to the $NDVI_{CV-MVC}$ since the BRDF results were used most frequently over less humid, lower biomass conditions.

The fractions of pixels over the globe for which the NDVI values were derived from either the BRDF-, CV-MVC-. or MVC-part of the MODIS algorithm were given for each consecutive composite period in Figure 5. The fraction of BRDF corrected pixels ranged between 20% and 35% globally. The beginning and end of the calendar year were more cloud-covered, resulting in

Figure 5. Temporal profile of the fractions of pixels for all continents, where the BRDF, CV-MVC, or MVC was used as part of the MODIS composite algorithm. All three fraction add up to one for a particular day of year (DOY).

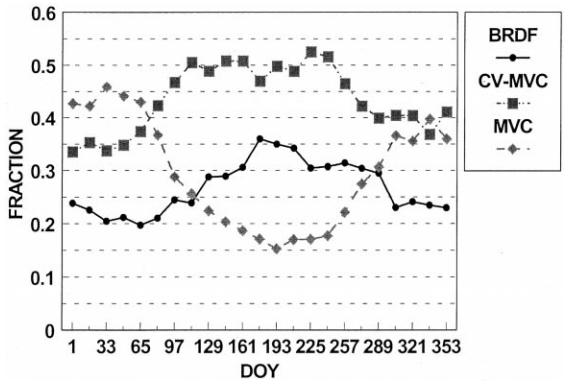

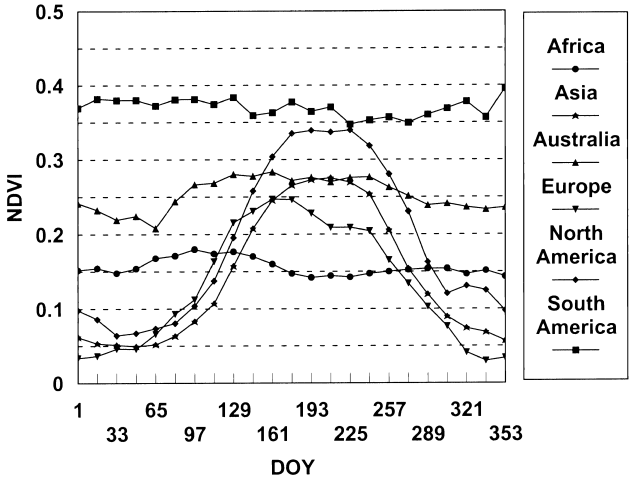

Figure 6. Continental NDVI profiles for the MODIS composite algorithm; AVHRR (8 km).

more MVC-based NDVI estimates. The CV-MVC algorithm was applied on 50% of the global pixels in the summer months and on about 35–40% of the global pixels during the winter months (Fig. 5). Initial MODIS-like VI composite results with SeaWiFS (Sea Viewing Wide Field of View Sensor) data (van Leeuwen et al., 1998) showed 50% of all global pixels to be standardized to a constant view angle (20°; the SeaWiFS tilt angle). Since SeaWiFS and AVHRR have equatorial crossing times of noon and afternoon respectively, it is anticipated that the MODIS morning crossing time will result in even more view angle standardized composite results.

Figure 6 shows seasonal profiles of the $NDVI_{MODIS}$ for each continent. The peak of the growing season is different for each continent (Fig. 6). The relative differences [100 $(NDVI_{MVC}-NDVI_{MODIS})/NDVI_{MVC}$] were computed for each continent and ranged between 1% and 24% for all 16-day composite periods during the 1989 AVHRR observations (van Leeuwen et al., 1997b).

Desert and Deciduous Broadleaf Forest Temporal VI Profiles

The relative accuracy of the MODIS-BRDF algorithm was evaluated through temporal NDVI, red, and NIR value profiles from pixels extracted from desert and deciduous broadleaf forest (Figs. 7 and 8). Although it was not the objective of this study to provide composited reflectance data, users will benefit from this byproduct of the vegetation index composite scenarios for numerous applications (classifications, change detection, maps). Figure 7a shows an example of a seasonal $NDVI_{MODIS}$ and $NDVI_{MVC}$ profiles, with the $NDVI_{MODIS}$ being equal or slightly lower then the $NDVI_{MVC}$. $NDVI_{MODIS}$ profiles are slightly smoother than the $NDVI_{MVC}$ profiles (Figs. 7a and 8a, 8b). The temporal red and NIR reflectance profiles (Fig. 7b) are following the same trend for both

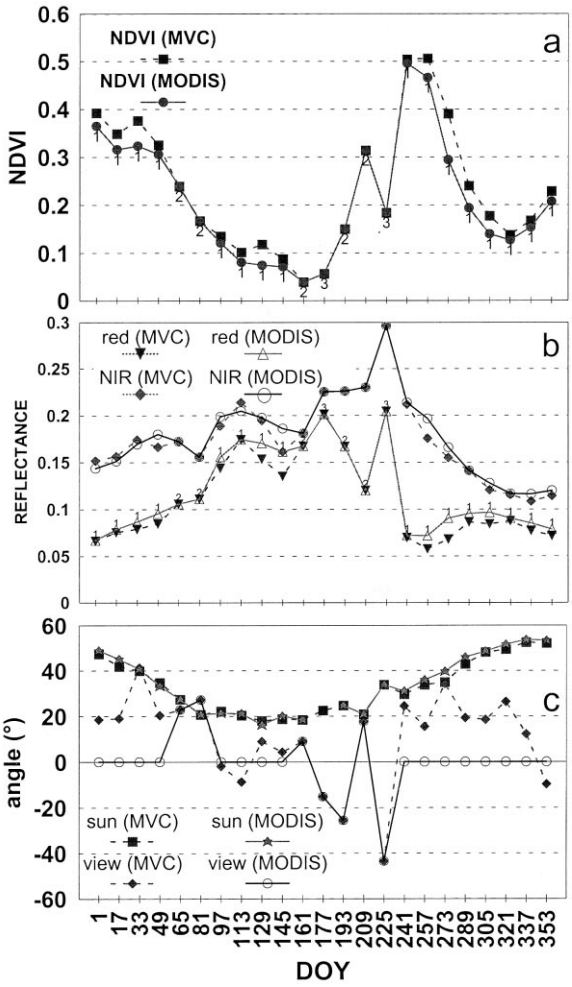

Figure 7. Example of temporal profiles of a) NDVI, b) red and NIR reflectance values, and c) sun and view zenith angles, for one pixel in a broadleaf deciduous (lat. 22.92°N, long. 75.98°E) forest [vegetation classification based on Kuchler's (1995) world natural vegetation map] for the MODIS and the MVC composite approaches using AVHRR data. For each composite period the MODIS composite method is indicated with a number in Figures 7a and 7b: 1—BRDF; 2—CV-MVC; 3—MVC.

MVC and MODIS composite methods. The combination of MODIS BRDF and CV-MVC composite methods performed well. The benefit of the MODIS approach is noticeable by the smaller range of view angles (Fig. 7c) and the associated smaller pixel sizes. The view angles associated with the CV-MVC are often equal to the MVC approach since there are not any better observations available. During DOYs 177 and 225 (Fig. 7), an unconstrained MVC was applied, since the cloud mask indicated that there were no cloud-free data available. In this case the reflectance values in both the red and NIR bands were higher then the reflectance values of the composite results before and after this particular example. Obvious discontinuities or artifacts due to the com-

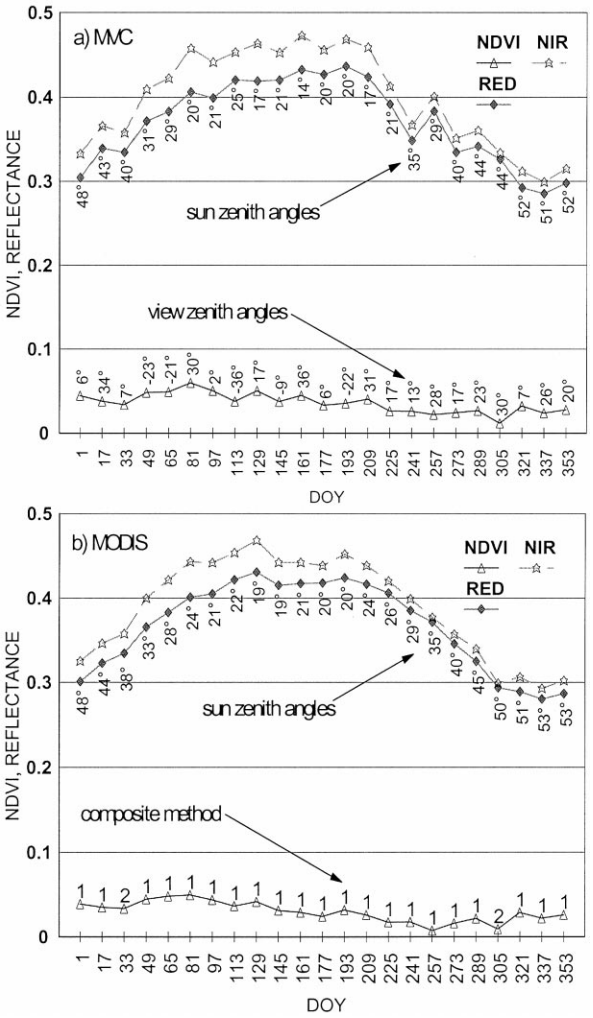

Figure 8. Example of temporal profiles of NDVI, red, and NIR reflectance values for one desert vegetation pixel (lat. 22.0°N, long. 27.15°E) [vegetation classification based on Kuchler's (1995) world natural vegetation map] for the a) MVC and b) MODIS composite approaches using AVHRR data. For each composite period the MODIS composite method is indicated with a number: 1—BRDF; 2—CV-MVC. The sun zenith angle and view zenith angle are also shown for each composite period. The negative and positive view angles are indicated for the respective backscatter and forward scatter view direction. The view zenith angle for the MODIS-BRDF corrected data is 0°.

bined use of two to three composite methods were not observed. The MVC and the MODIS-BRDF results (NDVI, red, and NIR reflectance values) were compared over a "desert" pixel in Figure 8. The red and NIR reflectance values increased with smaller solar zenith angles. The MODIS-BRDF model was applied almost every composite period, resulting in a slightly smoother temporal red and NIR reflectance and NDVI profiles (Fig. 8b), compared to the results of the MVC-approach (Fig. 8a).

Prototype Imagery of a MODIS VI

Figures 9 and 10 are prototype images of the global MODIS-NDVI and QA product for one 16-day composite period. The combination of MODIS BRDF and CV-MVC (constraint view angle–maximum value composite) composite methods performed well. Obvious discontinuities or artifacts due to the combined use of two to three composite methods were not observed. The pseudocolor image of the NDVI allows for fast visual examination of vegetation density and photosynthetically active regions of the world. The associated pseudocolor quality assurance (QA) image permits for quality checks of the algorithm, cloud cover persistence, and examination of the region with missing data.

Temporal and spatial QA and VI trend analysis will be a powerful tool to detect effects of climate change and monitor vegetation dynamics. Note that the BRDF correction is limited to the semiarid/arid regions, where cloud cover is less persistent than over other regions of the world. It is likely that the cloud cover will be less for the AM overpass time of MODIS in comparison with the afternoon overpass time of AVHRR. Consequently, the BRDF correction will be more frequently applied relative to the AVHRR PM data.

The performances of the MODIS and MVC composite algorithms were evaluated by quantifying and displaying the difference between the resulting $NDVI_{MODIS}$ values with those of $NDVI_{MVC}$ (Fig. 11). Although not displayed, the $NDVI_{MODIS}$ was subtracted from the $NDVI_{MVC}$ for all 23 16-day composites during 1989. Visual inspection of Figures 9, 10, and 11 indicated that the largest differences occurred among BRDF corrected pixels except for the deserts. The absolute difference was generally greater for the higher biomass pixels with higher NDVI values. This would indicate stronger anisotropic behavior for denser vegetation types. Subpixel cloud contamination in the "clear pixels," not detected by the CLAVR mask, could also reduce the NDVI values resulting from the BRDF model; however, this effect should be small since the BRDF-NDVI is weighted by at least five clear acquisitions. Nevertheless, an accurate

Figure 9. Global NDVI image (pseudocolor) using the MODIS VI composite algorithm (BRDF/CV-MVC/MVC approach).

Figure 10. Color-coded quality assurance flags for a Global NDVI composite using the MODIS approach (BRDF/CVMVC/MVC); MVC (pr) the cloud mask indicated the pixels to be probably cloudy; MVC (cl)=cloudy pixels; land surfaces without data were indicated with a dark color gray.

Figure 11. Difference image, where the $NDVI_{MODIS}$ was subtracted from the $NDVI_{MVC}$. The differences were color-coded with a range of intervals to bring out small differences between the two compositing scenarios. The interpretation of the NDVI difference image is complemented with the QA image (Fig. 10).

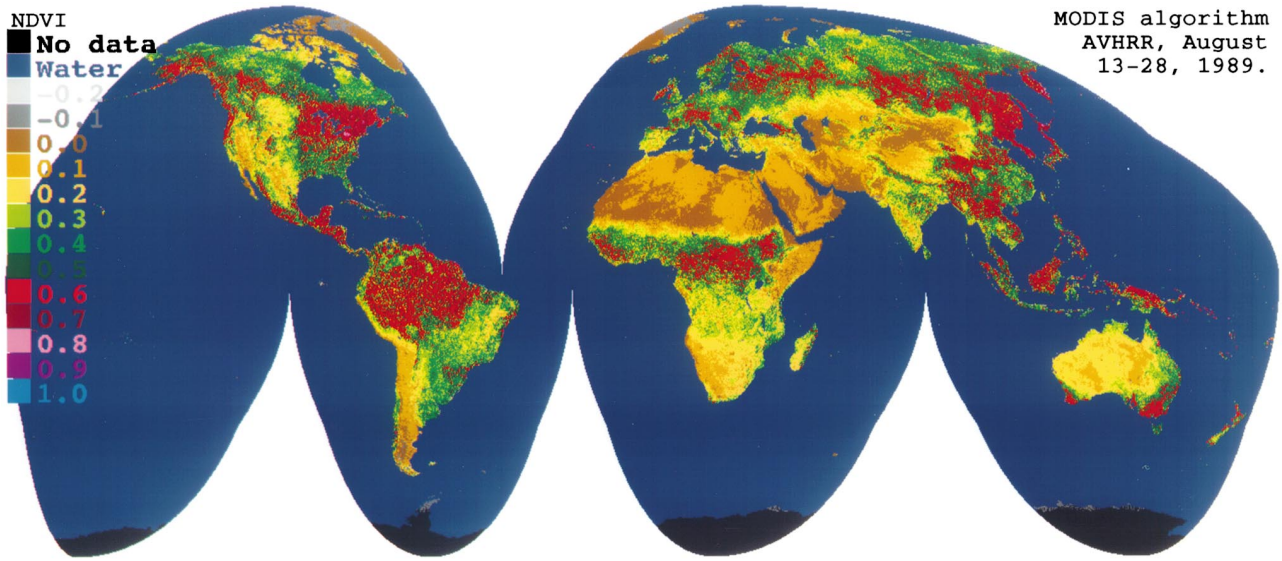

Figure 9.

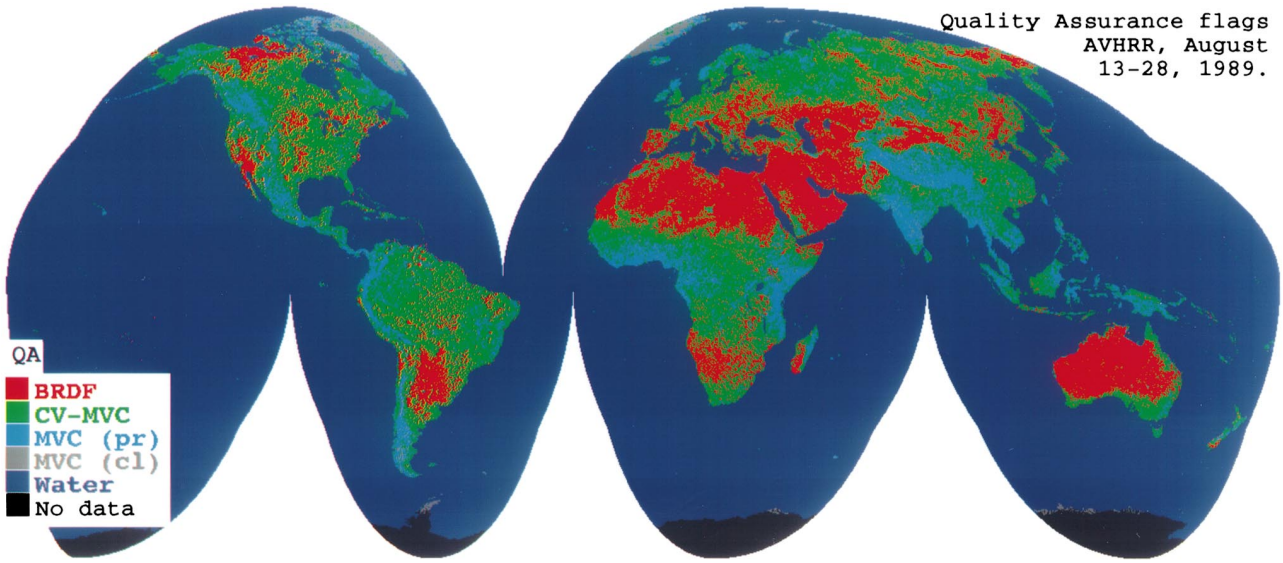

Figure 10.

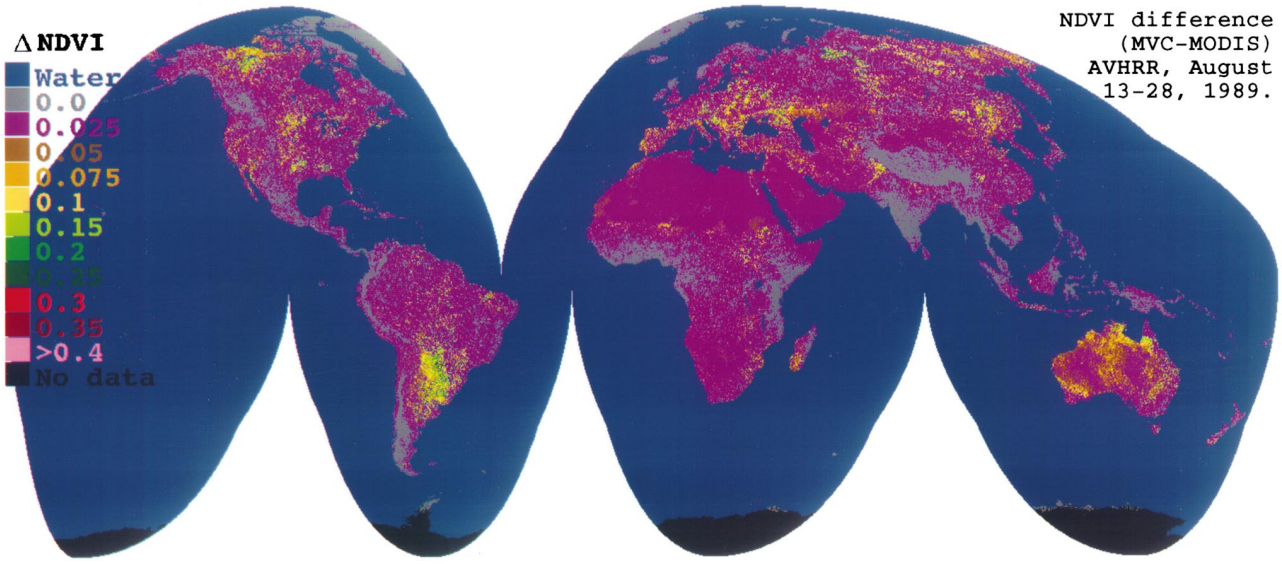

Figure 11.

cloud mask is critical for the use of BRDF models to standardize reflectance values to nadir view angles.

The MODIS algorithm essentially applies two separate but complementary composite scenarios: a BRDF scenario and a CV-MVC scenario. If the observations are of good quality, but limited to less then five observations, the view angles associated with these observations can be constrained to the ones closest to nadir. However, if the data integrity mask or cloud-mask indicated that all the observed data are not good, experience has shown that an unconstrained MVC approach can still "save" some observations that were identified as "bad" data. This situation quite often occurred over mountainous and snow and ice covered regions (Figs. 9 and 10) and during the winter months. More validation and research needs to be done on the CLAVR cloud mask to better discriminate regions of snow, ice, and clouds. Since the MODIS cloud mask product can make use of spectral bands specifically designed to detect clouds as well as the implementation of land cover specific algorithms, it is expected that the quality of the cloud mask will improve over the cloud mask for AVHRR data. In contrast to AVHRR, the MODIS daily surface reflectance product will not produce reflectance values for any observations affected by clouds. A so-called "fill value," for example, "−1000," will be substituted for all observations that are indicated to be cloud affected or have a bad integrity.

Although the resulting VI product can be traced to the input data, it is difficult to validate the cloudmask due to a lack of reliable information on cloud cover and its changes with time. It should be noted that the MODIS composite scenario can currently only be prototyped with AVHRR data. Global, daily, atmospherically corrected reflectance data, and cloud information cannot be produced with the current AVHRR satellite sensors which lack accurate calibration, geolocation, and atmospheric correction input parameters. Therefore, the global MODIS VI prototype with AVHRR data can only be tested taking into account the existing differences between the MODIS and AVHRR satellite characteristics and the data processing algorithms.

All AVHRR NIR values seem quite low compared to surface reflectance observations for these vegetation types from other sensors, for example, LANDSAT (Huete et al., 1997). This is mostly due to the aerosol and water vapor absorption for which the AVHRR data were not corrected. Therefore, all results presented are relative to the incomplete atmospheric correction and AVHRR sensor characteristics. Another difference between AVHRR and MODIS data is that MODIS data will consist of a variable number of observations per pixel and per day (the number of observations increase with higher latitudes due to overlapping orbits and the overlap of each scan, the so-called bow-tie effect), which all will be utilized in the compositing algorithm.

Because the AVHRR data only includes the red and NIR bands, the prototyping was limited to the NDVI. The enhanced vegetation indices (EVI) have been prototyped with LANDSAT Thematic Mapper data (Huete et al., 1997) and will be produced globally once the actual MODIS data becomes available. Where possible, atmospherically corrected AVHRR data (PATHFINDER II) and SeaWiFS data will be used to further investigate and prototype the MODIS vegetation index composite algorithm (van Leeuwen et al., 1998). SeaWiFS data is now available, but since it has no thermal bands, the determination of cloud affected observations will be challenging.

View Angle Distribution

The benefit of the MODIS compositing approach is noticeable by the smaller or equal view angles and the associated smaller pixel sizes. The view angle distribution of the MVC algorithm is more biased towards the forward scatter direction than the view angle distribution of the MODIS algorithm (Fig. 12). The strong peak at nadir view angles is due to the BRDF standardization of the reflectance factors to nadir. The view angle distribution of the CV-MVC algorithm is also less biased towards the forward scatter (positive angles) in comparison with the MVC algorithm as shown in Figure 13. As can be seen in Table 2, the sun zenith angles changed significantly depending on the continent (geolocation) and time of the year. The approximate day of the year where the sun angle reached its minimum and maximum were derived from the AVHRR (afternoon overpass) composited product. Future research will address more effective ways of standardizing reflectance observations with BRDF models to increase the spatial representation on a global scale.

Figure 12. Global view angle distribution (including all continents) for a 16-day composite period (13–28 August 28 1989) for the MODIS and MVC algorithms.

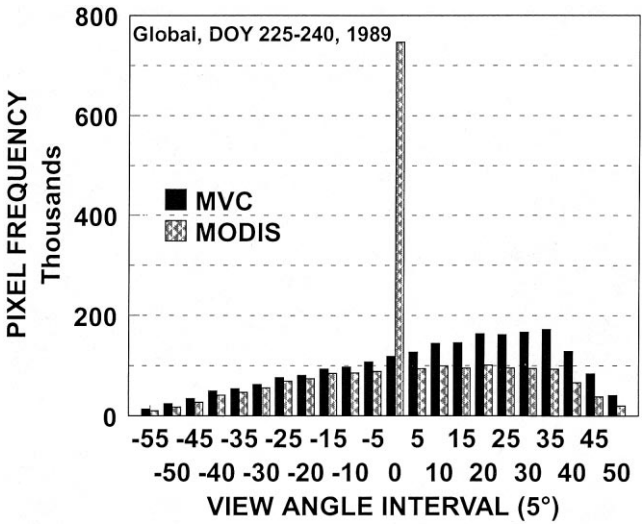

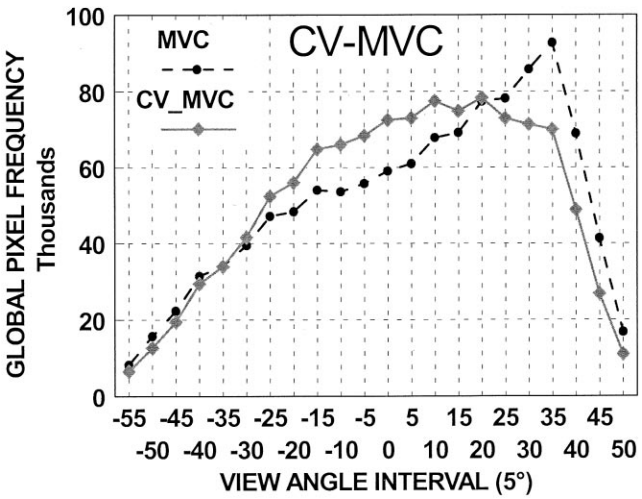

Figure 13. View angle distribution for all pixels where the CVMVC algorithm was applied (see green color in Fig. 10). The view angle distribution of the same pixels as a result of the MVC algorithm is shown as a comparison.

Alternative Composite Approaches

The MODIS/MISR BRDF production scheme will generate BRDF parameters and albedo every sixteen days with a 1 km spatial resolution with a required minimum of 10 cloud-free observations to be reliable (Strahler et al., 1996). The MODIS BRDF database is currently incompatible with the needs of the 250 m gridded MODIS NDVI product due to the coarser spatial and temporal resolutions of the BRDF product. Since the MODIS VI compositing algorithm has the specific aim of deriving nadir equivalent reflectance values, and not the complete BRDF (needed for albedo), five observations are considered sufficient for nadir interpolation. The feasibility of applying the BRDF product (1 km) to finer resolutions (250 m) (sharpening mode of the BRDF product) was investigated by van Leeuwen et al. (1997a) showing promising results for relatively homogeneous land cover types. The use of previous composite BRDF results or a historic BRDF database is also being investigated for situations where it is impossible to derive nadir reflectance values due to a limited number of observations (Leeuwen et al, 1997a; Wanner et al., 1997).

Table 2. The Maximum and Minimum Mean Solar Zenith Angles for Land and the Different Continents Based on the AVHRR Composited Data[a]

Continents	*Sun Angle (deg)*	
All (global)	33°	53°
South America	46°	33°
North America	30°	67°
Europe	28°	66°
Australia	51°	32°
Asia	27°	62°
Africa	26°	46°
DOY	161	337

[a] As expected, the approximate day of year (DOY) the minima and maxima occur, are during spring and fall.

Standardization of VI to nadir view and a certain sun angle is being investigated for a monthly CMG VI product. Monthly compositing would ensure sufficient input data for BRDF determination using inversion of a simple BRDF model (Rahman's; Rahman et al., 1993). The VI would be globally normalized to a constant solar-view geometry (possibly determined by the angle most sensitive to canopy biomass) at 0.25° spatial resolution (25 km). At the lower temporal resolution, this product would be catered towards modelers and those doing interannual comparisons. Local/regional work demanding more frequent data would probably rely on the 16-day level 3 VI as planned.

CONCLUSION

This article presented a description and evaluation of the current status of the MODIS vegetation index compositing algorithm. Vegetation indices have been shown to be an excellent tool to detect global and regional change and have been used to derive land cover classifications and vegetation state parameters. Because reflectance properties of the land surface are anisotropic in nature, vegetation indices, derived from bidirectional reflectance values, are strongly affected by the angular properties at which the target was viewed and illuminated. Retrieval of the bidirectional reflectance distribution function and angular standardization of these reflectance data are essential for the proper interpretation of vegetation index data and their derived parameters.

The MODIS instrument is currently planned for launch by NASA in the summer of 1999. However, it is expected that the full potential of the MODIS VI products will not be realized until the new millennium. Most product algorithms will need fine-tuning and several reprocessing steps to establish stable and well calibrated data time-series at multiple spectral and spatial resolutions. The improved capabilities of MODIS will offer the opportunity to cross-validate the historical and ongoing AVHRR-NDVI time series (since 1982) with the MODIS-NDVI time series. Especially the differences between the AVHRR and MODIS sensors in the spectral, radiometric, and spatial domain need to be translated to meet the needs of global change research. Biophysical parameters such as percent cover, biomass, fAPAR, and LAI, have been derived from the NDVI measured at variable view and sun angles. Standardizing these angular effects will also allow for more accurate derivations of biome specific or global biophysical parameters from VIs. Although the EVI was not prototyped in this case due to the lack of a blue band, the EVI will extend sensitivity

into dense vegetation types such as forests and agricultural areas while reducing the noise effects of canopy background and atmospheric aerosols (Justice et al., 1998).

The availability of MODIS VI data to the broader user community will be established by accessing and ordering data at the EOSDIS (Earth Observing System Data and Information System). EOSDIS will distribute the archived data sets using tape media, CD-ROM, and the network when possible. It is intended to publish a manual for the user community with recommendations and background information on the use and application of the MODIS vegetation indices.

There is some concern that the MODIS compositing approach, a combination of the BRDF and back-up MVC (maximum value composite) methods, will affect data purity and cause more discontinuities on a regional scale than a single criteria composite method (e.g., MVC). At this point, the MODIS approach has the advantage over the MVC approach through standardization of view angles and emphasis on the selection of nadir (finest spatial resolution) observations. However, the MODIS approach is more adversely affected by cloud and atmospheric effects than the MVC. The selection of the maximum NDVI tends to mask the natural vegetation variations in more densely vegetated areas due to saturation effects. A final evaluation of the MODIS composite approach will be based on the quality of the actual MODIS data, product evaluations and user community requirements.

Since many uncertainties remain as to how the actual MODIS instrument and the developed algorithms are going to perform, some flexibility is being built into the current MODIS VI compositing algorithm, that allows for unexpected (e.g., unreliable georegistration, cloud mask, and atmospheric correction) data input flows. The compositing algorithm thresholds and parameters can be relaxed or tightened depending on the quality of the data. For instance, immediately after launch, the BRDF module of the compositing algorithm can be switched off to accommodate less ideal data due to unsuccessful cloud-masking or inaccurate day to day georegistration. The quality of the MODIS data processing algorithms and the MODIS specific spatial, temporal, spectral, and radiometric quality of the data after the initial postlaunch processing will greatly determine if all the MODIS compositing goals can be achieved.

The following conclusions can be drawn based on prototyping the MODIS vegetation index approach with AVHRR data:

- A simple BRDF model and few observations ($\geqslant 5$) per pixel were needed to standardize the NDVI to nadir view angles and thus improve the interpretation of the anisotropic VIs.
- The Walthall BRDF model was successfully used in prototyping global MODIS-EOS/NDVI composite scenarios with AVHRR data.
- Results of a BRDF approach are more representative of vegetation changes over a 16-day period than the MVC approach, because it incorporates all "good" observations and changes during a 16-day period.
- The present MODIS-BRDF composite scenario automatically extrapolates to finer (nadir) spatial resolutions.
- A reliable cloud mask is crucial to the BRDF component of the MODIS compositing algorithm to exclude observations of cloud affected pixels.
- A back-up composite algorithm was needed for the pixels with a limited number of "good" observations since the BRDF model cannot be reliably inverted if the Earth's surface is frequently covered with clouds.
- On a continental scale, the MVC based NDVI values were 1–30% higher than the NDVI values derived from the MODIS algorithm.

Since the vegetation indices are radiometric measures of the spatial and temporal variations of vegetation biophysical properties, validation activities will focus on the relationship of the radiometric and biophysical changes of the land surface and incorporate multiangular measurements as well. Research and validation activities are in progress to demonstrate the utility of the MODIS vegetation indices to improve the understanding of the Earth system and its dynamics due to interactions between climate and land processes and human activity.

Data used by the authors in this study included data produced through funding from the Earth Observing System Pathfinder program of NASA's Mission to Planet Earth in cooperation with the National Oceanic and Atmospheric Administration. The data were provided by the Earth Observing System Data and Information System, Distributed Active Archive Center at Goddard Space Flight Center which archives, manages, and distributes this data set. This research was supported by MODIS Contract NAS5-31364 (A. R. Huete).

REFERENCES

Agbu, P. A., and James, M. E. (1994), *The NOAA/NASA Pathfinder AVHRR Land Data Set User's Manual*, Goddard Distributed Active Archive Center, NASA, Goddard Space Flight Center, Greenbelt.

Ackerman, S., Strabala, K., Menzel1, P., et al. (1996), Discriminating Clear-Sky from Cloud with MODIS Algorithm Theoretical Basis Document V3, http://eospso.gsfc.nasa.gov/atbd/modistables. html.

Archard, F., Malingreau, J. P., Phulpin, T., et al. (1994), A mission for global monitoring of the continental biosphere, VEGETATION International Users Committee Secretariat, Joint Research Centre, Institute for Remote Sensing Applications, I-21020 ISPRA (Va), Italy, http://www-vegetation.cst.cnes.fr:8050/.

Asrar, G., Fuchs, M., Kanemasu, E. T., and Hatfield, J. L. (1984), Estimating absorbed photosynthetic radiation and leaf area index from spectral reflectance in wheat. *Agron. J.* 76:300–306.

Asrar, G., Myneni, R. B., and Choudhury, B. J. (1992), Spatial heterogeneity in vegetation canopies and remote sensing of absorbed photosynthetically active radiation: a modeling study. *Remote Sens. Environ.* 41:85–101.

Baret, F., and Guyot, G. (1991), Potentials and limits of vegetation indices for LAI and APAR assessment. *Remote Sens. Environ.* 35:161–173.

Cihlar, J. C., Ly, H., Li, Z., Chen, J., Pokrant, H., and Huang, F.(1997), Multitemporal, multichannel AVHRR data sets for land biosphere studies—artifacts and corrections. *Remote Sens. Environ.* 60:35–57.

Cihlar, J., Manak, D., and Voisin, N. (1994a), AVHRR bidirectional reflectance effects and compositing. *Remote Sens. Environ.* 48:77–88

Cihlar, J., Manak, D., and D'Iorio, M., (1994b), Evaluation of compositing algorithms for AVHRR data over land. *IEEE Trans. Geosci. Remote Sens.* 32:427–437.

Deering, D. W., and Leone, 1986. A sphere-scanning radiometer for rapid directional measurements of sky and ground radiance. *Remote Sens. Environ.* 19:1–24.

Eidenshink, J. C., and Faundeen, J. L. (1994), The 1km AVHRR global land data set: first stages in implementation. Int. J. Remote Sensing, 15(17), pp. 3443–3462.

Fung, Y., Tucker, C. J. and Prentice, K. C. (1987), Application of Advanced Very High Resolution Radiometer Vegetation Index to Study Atmosphere–Biosphere Exchange of CO_2. J. Geoph. Res., 92, 2999–3015.

Goward, S. N., and Huemmrich, K. F. (1992), Vegetation canopy PAR absorptance and the normalized difference vegetation index: an assessment using the SAIL model. *Remote Sens. Environ.* 39:119–140.

Goward, S. N., Markham, B., Dye, D. G., Dulaney, W., and Yang, J.(1991), Normalized difference vegetation index measurements from the Advanced Very High Resolution Radiometer. *Remote Sens. Environ.* 35:257–277.

Goward, D. G., Turner, S., Dye, D. G., and Liang, J., (1994), University of Maryland improved global vegetation index. *Int. J. Remote Sens.* 15:3365–3395.

Gutman, G. G. (1991), Vegetation indices from AVHRR: an update and future prospect. *Remote Sens. Environ.* 35:121–136.

Holben, B. N. (1986), Characterization of maximum value composites from temporal AVHRR data. *Int. J. Remote Sens.* 7:1417–1434.

Hooker, S. B., Esaias, W. E., Feldman, G. C., Gregg, W. W., and McClain, C. R. (1992), An overview of SeaWiFS and ocean color, NASA Tech. Memo. 104566, Vol. 1 (S. B. Hooker and E. R. Firestone, Eds.), NASA Goddard Space Flight Center, Greenbelt, MD, 24 pp.

Huete, A. R., Liu, H. Q., Batchily, K., and van Leeuwen, W. (1997), A comparison of vegetation indices over a global set of TM images for EOS-MODIS. *Remote Sens. Environ.* 59:440–451.

Huete, A. R., Justice, C. O., and van Leeuwen, W. J. D. (1999), MODIS Vegetation Index, Algorithm Theoretical Basis Document, http://modarch.gsfc.nasa.gov/MODIS/ATBD/atbd_mod13.pdf.

James, M. D., and Kalluri, S. N. V. (1994), The Pathfinder AVHRR land data set: an improved coarse resolution data set for terrestrial monitoring. *Int. J. Remote Sens.* 15:3347–3363.

Justice, C. O., Townshend, J. R. G., Holben, B. N., and Tucker, C. J. (1985), Analysis of the phenology of global vegetation using meteorological satellite data. *Int. J. Remote Sens.* 6:1271–1318.

Justice, C., Hall, D., Salomonson, V., et al. (1998), The Moderate Resolution Imaging Spectroradiometer (MODIS): land remote sensing for global change research. *IEEE Trans. Geosci. Remote Sens.* 36:1228–1249

Kimes, D. S., Holben, B. N., Tucker, C. J., and Newcomb, W. W. (1984), Optimal directional view angles for remote-sensing missions. *Int. J. Remote Sens.* 5:887–908.

Kimes, D. S., Newcomb, W. W., Tucker, C. J., et al. (1985), Directional reflectance factor distribution for cover types of northern Africa. *Remote Sens. Environ.* 18:1–19.

Kuchler, A. W. (1995), Natural vegetation map. In *Rand McNally Goode's World Atlas*, 19th ed. (E. B. Espenshade, J. C. Hudson, and J. L. Morrison, Eds.), Rand McNally, Chicago, pp. 18–19.

Lucht, W. (1998), Expected retrieval accuracies of bidirectional reflectance and albedo from EOS-MODIS and MISR angular sampling. *J. Geophys. Res.* 103(D8):8763–8778.

Meyer, D., Verstraete, M., and Pinty, B. (1995), The effect of surface anisotropy and viewing geometry on the estimation of NDVI from AVHRR. *Remote Sens. Rev.* 12:3–27.

Miura, T. Huete, A. R., van Leeuwen, W. J. D., and Didan, K. (1998), Vegetation detection through smoke-filled AVIRIS images: an assessment using MODIS band passes. *J. Geophys. Res.* 103:32,001–32,011.

Moody, A. and Strahler, A. H. (1994), Characteristics of composited AVHRR data and problems in their classification. *Int. J. Remote Sens.* 15:3473–3491.

Morisette, J. T., Privette, J. L., Justice, C. O., and Running, S. W. (1998), MODIS Land Validation Plan; MODIS Land Discipline Team, http://modarch.gsfc.nasa.gov/MODIS/LAND/VAL/land_val_plan.pdf.

Nakajima, T. Y., Nakajima, T., Nakajima, M., et al. (1998), Optimization of the Advanced Observing Satellite Global Imager channels by use of radiative transfer calculations. *Appl. Opt.* 37(15):3149–3163.

Price, J. C. (1987), Calibration of satellite radiometers and the comparison of vegetation indices. *Remote Sens. Environ.* 21:419–422.

Prince, S. D. (1991), A model of regional primary production for use with coarse resolution satellite data. *Int. J. Remote Sens.* 12:1313–1330.

Privette, J. L. Myneni, R. B., Emery, W. J., and Hall, F. G. (1996), Optimal sampling conditions for estimating grassland parameters via reflectance model inversions. *IEEE Trans. Geosci. Remote Sens.* 34:272–284.

Privette, J. L., Eck, T. F., and Deering, D. W. (1997), Estimating spectral albedo and nadir reflectance through inversion of simple BRDF models with AVHRR/MODIS-like data. *J. Geophys. Res.* 102(D24):29,529–29,542.

Qi, J., and Kerr, Y. (1997), On current compositing algorithms. *Remote Sens. Rev.* 15:235–256.

Qi, J., Huete, A. R., Hood, J., and Kerr, Y. (1994), Compositing multi-temporal remote sensing data sets. In *PECORA 11*,

Symposium on Land Information Systems, Sioux Falls, August 1993, American Society for Photogrammetry and Remote Sensing, Bethesda, MD, pp. 206–213.

Rahman, H., Pinty, B., and Verstraete, M. M. (1993), Coupled surface-atmosphere reflectance (CSAR) model 2. Semiemperical surface model usable with NOAA AVHRR. *J. Geophys. Res.* 89(D11):20,791–20,801.

Raich, J. W., and Schlesinger, W. H. (1992), The global carbon dioxide flux in soil respiration and its relationship to vegetation and climate. *Tellus* 44B:81–99.

Roujean, J. L., Leroy, M., Podaire, A., and Deschamps, P. Y. (1992), Evidence of surface reflectance bidirectional effects from a NOAA/AVHRR multi-temporal data set. *Int. J. Remote Sens.* 13:685–698.

Roy, D. P. (1997), Investigation of the maximum normalized difference vegetation index (NDVI) and the maximum surface temperature (T_s) AVHRR compositing procedures for the extraction of NDVI and T_s over forest. *Int. J. Remote Sens.* 18:2383–2401.

Running, S. W., and Nemani, R. R. (1988), Relating seasonal patterns of the AVHRR vegetation index to simulated photosynthesis and transpiration of forest in different climates. *Remote Sens. Environ.* 24:347–367.

Salomonson, V. V., Barnes, W. L., Maymon, P. W., Montgomery, H. E., and Ostrow, H. (1989), MODIS: advanced facility instrument for studies of the earth as a system. *IEEE Trans. Geosci. Remote Sens.* 27:145–153.

Sellers, P. C. (1985), Canopy reflectance, photosynthesis and transpiration. *Int. J. Remote Sens.* 6:1335–1372.

Sellers, P. J., Tucker, C. J., Collatz, G. J., et al. (1994), A global 1°*1° NDVI data set for climate studies. Part 2—the adjustment of the NDVI and generation of global fields of terrestrial biophysical parameters. *Int. J. Remote Sens.* 15: 3519–3545.

Stowe, L. L., McClain, E. P., Carey, R., et al. (1991), Global distribution of cloud cover derived from NOAA/AVHRR operational satellite data. *Adv. Space Res.* 3:51–54.

Strahler, A., Li, X., Liang, S., Muller, J.-P., Barnsley, M., Lewis, P. (1996), MODIS BRDF/Albedo Product: ATBD Version 4, http://eospso.gsfc.nasa.gov/atbd/modistables.html.

Tans, P. P., Fung, I. Y., and Takahashi, T. (1990), Observational constraints on the global atmosphere CO2 budget. *Science* 247:1431–1438.

Teillet, P. M., Staenz, K., and Willams, D. J. (1997), Effects of spectral, spatial, and radiometric characteristics on remote sensing vegetation indices of forested regions. *Remote Sens. Environ.* 61:139–149.

Townshend, J. R. G. (1994), Global data sets for land applications from the AVHRR: an introduction. *Int. J. Remote Sens.* 15:3319–3332.

Townshend, J. R. G., Justice, C. O., Gurney, C., and McManus, J. (1992), The impact of misregistration on the detection of changes in land cover., *IEEE Trans. Geosci. Remote Sens.* 30:1054–1060.

Townshend, J. R. G., Justice, C., Li, W., Gurney, C., and McManus, J. (1991), Global land cover classification by remote sensing: present capabilities and future possibilities. *Remote Sens. Environ.* 35:243–256.

Tucker, C. J., and Sellers, P. J. (1986), Satellite remote sensing of primary productivity. *Int. J. Remote Sens.* 7:1395–1416.

van Leeuwen, W. J. D., Huete, A. R., Duncan, J., and Franklin, J. (1994), Radiative transfer in shrub savanna sites in Niger—preliminary results from HAPEX-II-Sahel: 3. Optical dynamics and vegetation index sensitivity to biomass and plant cover. *Agric. For. Meteorol.* 69:267–288.

van Leeuwen, W. J. D., Huete, A. R., Jia, S., and Walthall, C. L. (1996), Comparison of vegetation index compositing scenarios: BRDF versus maximum VI approaches. *IEEE–IGARSS'96*, Lincoln NE, IEEE, New York, Vol. 3, pp. 1423–1425.

van Leeuwen, W. J. D., Huete., A. R., Didan, K., and Laing, T. (1997a), Modeling bi-directional reflectance factors for different land cover types and surface components to standardize vegetation indices. In *Proceedings of the 7th Int. Symposium on Physical Measurements and Signatures in Remote Sensing*, Courcheval, France; 7–11 April, (G. Guyot and T. Phulpin, Eds.), A.A. Balkema, Rotterdam, pp. 373–380.

van Leeuwen, W. J. D., Laing, T. W., and Huete, A. R. (1997b), Quality assurance of global vegetation index compositing algorithms using AVHRR data. In *IEEE–IGARSS'97*, Singapore, IEEE, New York, pp 341–343.

van Leeuwen, W. J. D., Huete, A. R., and Laing, T. (1998), Evaluation of the MODIS vegetation Index Compositing algorithm using SeaWiFS data. In *IEEE–IGARSS'98*, Seattle, IEEE, New York.

Vermote, E., Tanré, D., Deuzé, J. L., Herman, M., and Mocrette, J. J. (1997a), Second simulation of the satellite signal in the solar spectrum: an overview. *IEEE Trans. Geosci. Remote Sens.*. 35(3):675–686.

Vermote, N., El Saleous, N., Justice, C. O., et al. (1997b), Atmospheric correction of visible to middle-infrared EOS-MODIS data over land surfaces: background, operational algorithm and validation. *J. Geophys. Res.* 102(D14):17,131–17,141.

Vierling, L. A., Deering, D. W., and Eck, T. F. (1997), Differences in Arctic tundra vegetation type and phenology as seen using bidirectional radiometry in the early growing season. *Remote Sens. Environ.* 60:71–82.

Viovy, N., Arino, O., and Belward, A. S. (1992), The best index slope extraction (BISE): a method for reducing noise in NDVI time series. *Int. J. Remote Sens.* 13:1585–1590.

Walter-Shea, E. A., Privette, J. L., Cornell, D., Mesarch, M. A., and Hays, C. J. (1997), Relations between spectral vegetation indices and leaf area and absorbed radiation in alfalfa. *Remote Sens. Environ.* 61:162–177.

Walthall, C. L., Norman, J. M., Welles, J. M., Campbell, G., and Blad, B. L. (1985), Simple equation to approximate the bi-directional reflectance from vegetative canopies and bare soil surfaces. *Appl. Opt.* 24:383–387.

Wanner, W., Strahler, A. H., Hu, B., et al. (1997), Global retrieval of bidirectional reflectance and albedo over land from EOS MODIS and MISR data: theory and algorithm. *J. Geophys. Res.* 102(D14):17,143–17,161.

Wolfe, R. E., Roy, D. P., and Vermote, E. (1998), MODIS land data storage, gridding, and compositing methodology: Level 2 grid. *IEEE Trans. Geosci. Remote Sens.* 36:1324–1338.

Wu, A., Li, Z., and Cihlar, J. (1995), Effects of land cover type and greenness on advanced very high resolution radiometer bidirectional reflectances: analysis and removal. *J. Geophys. Res.* 100(D5):9179–9192.